Implications for the Spectroscopic Assignment of Vanadium Biomolecules: Structural and Spectroscopic Characterization of Monooxovanadium(V) Complexes Containing Catecholate and Hydroximate Based Noninnocent Ligands

Charles R. Cornman, Gerard J. Colpas, James D. Hoeschele, Jeff Kampf, and Vincent L. Pecoraro*

Contribution from the Willard H. Dow Laboratory, Department of Chemistry, University of Michigan, Ann Arbor, Michigan 48109-1055. *Received June 1, 1992*

Abstract: Forty-one compounds of the general formula $V^{V}OLL'$, where L is a tridentate ligand (HSALIMH = [4-(2-salicylideneaminato)ethyl]imidazole; H_2SHED = *N*-(salicylideneaminato)-*N'*-(2-hydroxyethyl)ethylenediamine; HENSAL = *N*-(salicylideneaminato)ethylenediamine) and L' is a bidentate, noninnocent ligand (e.g., catechol (H_2CAT), pyrogallol (H_2PYR), or salicylhydroxamic acid (H_2SHI)) have been prepared and spectroscopically characterized. Three of these novel complexes have been structurally characterized by X-ray crystallography [$V^{V}O$(HSHED)(CAT), **1**, $V^{V}O$(SALIMH)(CAT), **3**, $V^{V}O$(HSHED)(SHI), **35**] which allows for a direct comparison of the coordination environments of $(V^{IV}O)^{2+}$ and $(V^{V}O)^{3+}$ with nearly identical ligand sets. The complexes VO(SALIMH)L' provide a direct test for a model for the enzyme vanadium bromoperoxidase that has coordinated imidazole, a single, terminal oxo ligand and oxygen donors that may be part of a noninnocent ligand. Furthermore, one can directly ascertain the effects of substituting primary or secondary amines for imidazole in an isostructural environment by comparing the properties of VO(HSHED)L' and VO(ENSAL)L'. Previously reported $V(O)O_3N_2$ compounds have shown chemical shifts in a narrow range between 300 and 600 ppm upfield of $VOCl_3$. In contrast, these $V^{V}OLL'$ complexes cover nearly 1200 ppm and can have resonances as much as 600 ppm *downfield* of $VOCl_3$. This unprecedented shift range and location is a direct consequence of the coordinated noninnocent ligands. The observed chemical shifts linearly correlate with the inverse energies of the ligand-to-metal charge-transfer bands in the visible and near infrared spectrum, and, therefore, a modification of Ramsey theory has been applied to extract the absolute shielding of these compounds. By extension, the absolute shielding of vanadium in the bromoperoxidase and vanadium transferrin can be inferred. This shielding scale indicates that for vanadium bromoperoxidase the temperature independent shielding factor σ^{p} is very small relative to most V(V) complexes implying that noninnocent ligands which have a large σ^{p} are almost certainly not involved in the coordination sphere of the metal in this enzyme. Crystal data: **1**, monoclinic, $P2_1/n$, a = 13.660 (9) Å; b = 6.483 (4) Å; c = 19.18 (1) Å; β = 96.69 (6)°; V = 1681 (2) Å^3; Z = 4. For 3527 data collected between $5 \le 2\theta \le 50°$ and 2569 data $> 0.6\sigma(F)$ the structure refined to R_1 = 0.063 (R_2 = 0.059); **3**, triclinic, $P\bar{1}$, a = 6.773 (1) Å; b = 10.717 (2) Å; c = 12.150 (4) Å; α = 98.40 (2)°; β = 92.13 (2)°; γ = 94.05 (2)°; V = 862.8 (4) Å^3; Z = 2. For 3427 data collected between $5 \le 2\theta \le 50°$ and 2860 data $> 0.6\sigma(I)$ the structure refined to R_1 = 0.042 (R_2 = 0.057); **35**, monoclinic, $P2_1/n$, a = 10.569 (3) Å; b = 11.698 (4) Å; c = 15.498 (4) Å; β = 98.85 (2)°; V = 1882.6 (8) Å^3; Z = 4. For 3840 data collected between $5 \le 2\theta \le 50°$ and 2764 data $> 0.6\sigma(F)$ the structure refined to R_1 = 0.068 (R_2 = 0.058).

Introduction

Despite the fact that mammalian vanadium concentrations are at the nano- to picomolar level, several lower organisms have a requirement for this element which is considerably more pronounced.[1,2] Ascidians (sea squirts) accumulate vanadium at levels up to 10^7-fold over their marine environment,[3] and the mushroom *Amanita muscaria* accumulates vanadium to produce the natural product amavadin.[4] Two enzymes have recently been isolated with a unique requirement for vanadium: (1) an alternative nitrogenase from several species of *Azotobacter*[5] and (2) a haloperoxidase from many marine algae.[6] The ligands pyrogallol (hydroxy catechol) and *N*-hydroxylamine–diisopropionic acid are present in the tunicates and *A. muscaria*, respectively, and may be coordinated to the metal center in the native systems. Although the composition of the metal coordination sphere in the vanadium bromoperoxidases is unknown at present, the anomalous ^{51}V NMR chemical shift indicates a novel coordination environment. Since vanadium bromoperoxidase is a rare example of a non-heme haloperoxidase, the peroxidase mechanism, which is inherently dependent on the electronic structure of the active site, is of considerable interest.

To date, no X-ray crystal structures have been presented for vanadium complexes isolated from natural sources. Vanadium bromoperoxidases have been studied by X-ray absorption,[7] electron paramagnetic resonance,[8] electronic,[6] and ^{51}V NMR spectroscopies.[9] These have been used to probe the structure of the metal site in these metallobiomolecules. Further, both EPR for vanadium(IV) and NMR for vanadium(V) have been utilized to study metal binding sites in vanadium substituted proteins such as bovine serum albumin and transferrin.[10,11] These studies have been especially useful in differentiating multiple binding sites in proteins such as the N and C terminal iron binding sites in transferrin. Specific assignment of the ligands which are coordinated to the metal center is a more difficult task. For this, one must understand

(1) For recent reviews of biologically relevant vanadium chemistry, see: (a) *Vanadium in Biological Systems*, Chasteen, N. D., Ed.; Kluwer Academic Publishers: Dordrecht, The Netherlands, 1990. (b) Butler, A.; Carrano, C. J. *Coord. Chem. Rev.* **1991**, *109*, 61. (c) Rehder, D. *Angew. Chem., Int. Ed. Engl.* **1991**, *30*, 148.

(2) Nielsen, H. F.; Othus, E. O. In *Vanadium in Biological Systems*, Chasteen, N. D., Ed.; Kluwer Academic Publishers: Dordrecht, The Netherlands, 1990; p 51.

(3) (a) Henze, M. *Hoppe-Seyer's Z. Physiol. Chem.* **1911**, *72*, 494. (b) Boyd, D. W.; Kustin, K. *Adv. Inorg. Biochem.* **1984**, *6*, 311. (c) Kustin, K.; McCleod, G. C.; Gilbert, T. R.; Briggs, L. B. R. 4th, *Struct. Bonding* **1983**, *53*, 139.

(4) (a) Bayer, E.; Kneifel, H. *Z. Naturforsch.* **1972**, *27B*, 207. (b) Kneifel, H.; Bayer, E. *Angew. Chem., Int. Ed. Engl.* **1973**, *12*, 508.

(5) (a) Robson, R. L.; Eady, R. R.; Richardson, T. H.; Miller, R. W.; Hawkins, M.; Postgate, J. R. *Nature* **1986**, *322*, 388. (b) Hales, B. J.; Case, E. P.; Morningstar, J. E.; Dzeda, M. F.; Mauterer, L. A. *Biochemistry* **1986**, *25*, 7251.

(6) (a) Vilter, H. *Bot. Mar.* **1983**, *26*, 429. (b) Vilter, H. *Bot. Mar.* **1983**, *26*, 451. (c) de Boer, E.; Tromp, M. G. M.; Plat, H.; Krenn, B. E.; Wever, R. *Biochim. Biophys. Acta* **1986**, *872*, 104. (d) Soedjak, H. S.; Butler, A. *Biochemistry* **1990**, *29*, 7974.

(7) Arbor, J. M.; de Boer, E.; Garner, C. D.; Hasnain, S. S.; Wever, R. *Biochemistry* **1989**, *28*, 7968.

(8) de Boer, E.; Boon, K.; Wever, R. *Biochemistry* **1988**, *27*, 1629.

(9) (a) Vilter, H.; Rehder, D. *Inorg. Chim. Acta* **1987**, *136*, L7. (b) Rehder, D.; Vilter, H.; Duch, A.; Preibsch, W.; Weidemann, C. *Recl. Trav. Chim. Pays-Bas* **1987**, *106*, 408.

(10) Chasteen, N. D. In *Biological Magnetic Resonance*; Berliner, L. J., Reuben, J. Eds.; Plenum Press: New York, 1981; Vol. 3, pp 53–119.

(11) Butler, A.; Eckert, H. *J. Am. Chem. Soc.* **1989**, *111*, 2802.

0002-7863/92/1514-9925$03.00/0

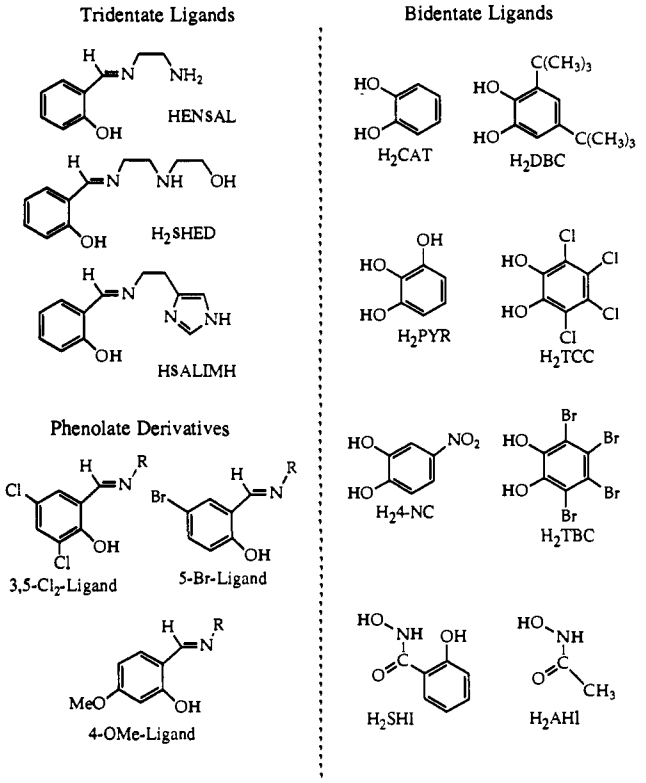

Figure 1. The ligands used in this study.

how each ligand modifies the magnetic field at the observed nucleus and how these modifications affect the experimentally observable parameters such as chemical shift and g value. Accumulation of data for a large number of compounds has led to the development of emperical relationships between spectroscopic observables and the local metal environment. Chasteen has shown a correlation between ligand (O or N donor) type and number and the g and A values for vanadium(IV) complexes.[10] Rehder has proposed a relationship between the vanadium-51 NMR chemical shift and the sum of the ligand electronegativities for a large, yet incomplete, set of coordination complexes.[12]

Empirical and semiquantitative relationships between the NMR chemical shift and electronic properties of the metal complexes, such as the energy of electronic transitions, have been advanced for most NMR observable nuclei.[13] These correlations are based on the theoretical treatment of the chemical shift presented by Ramsey in the early 1950s for molecules without intrinsic spin or orbital angular momentum.[14] According to this treatment, the total chemical shielding, σ, is a combination of diamagnetic and temperature independent paramagnetic contributions as shown in eq 1. Since σ^d is essentially constant for each nuclide, the

$$\sigma = \sigma^d + \sigma^p \quad (1)$$

chemical shift observed by the NMR technique is dependent on changes in the paramagnetic shielding term, σ^p, which are associated with changes in the electronic structure of the different molecules being examined. Based on this electronic dependence, one might expect complexes of common amino acid donor ligands such as imidazole, phenolate, or alkoxide to have significantly different chemical shifts compared to the more novel donors such as catechol derivatives, found in ascidians, or hydroxylamine derivatives, present in *A. muscaria*. These ligand types are known to form metal complexes with low-energy charge-transfer transitions which can dramatically affect the electronic environment at the metal nucleus and are thus described hereafter as noninnocent ligands. Molybdenum complexes of noninnocent ligands have novel spectroscopic properties which are directly related to the coordination of the noninnocent ligand as shown by Schultz and co-workers.[15] To the best of our knowledge, the metal centers in vanadium(V) complexes of these ligand types have not been examined by nuclear magnetic resonance spectroscopy except as a fingerprint technique.

To increase our understanding of the relationship between the chemical shift of the metal nucleus and the structural/electronic properties of the metal complex, we have undertaken the synthesis and characterization of a series of vanadium complexes that contain both innocent and noninnocent ligands. This series of six-coordinate monooxovanadium(V) complexes contain meridional tridentate ligands, shown in Figure 1, which maintain phenolato and iminato coordination and vary the third donor using primary and secondary amines or imidazole nitrogen atoms. The remaining two coordination positions are satisfied using a noninnocent, bidentate ligand derived from catechol or hydroxamic acids. These complexes exhibit low-energy ligand-to-metal charge-transfer transitions that significantly affect the spectroscopy observed for the complexes.

Table I. Summary of Crystallographic Data for Compounds **1**, **3**, and **35**

compound	**1**	**3**	**35**
mw	382.29	389.29	425.31
space group	$P\bar{1}$	$P2_1/n$	$P2_1/n$
a (Å)	6.773 (1)	13.660 (9)	10.569 (3)
b (Å)	10.717 (2)	6.483 (4)	11.698 (4)
c (Å)	12.150 (4)	19.18 (1)	15.498 (4)
α (deg)	98.40 (2)		
β (deg)	92.13 (2)	96.69 (6)	98.85 (2)
γ (deg)	94.05 (2)		
V (Å^3)	862.8 (4)	1681 (2)	1882.6 (8)
Z	2	4	4
μ (cm^{-1})	5.84	5.98	5.44
ρ_{cal} (g/cm^3)	1.471	1.537	1.500
ρ_{obs} (g/cm^3)	1.46 (1)	1.50 (2)	1.49 (1)
cryst size (mm)	0.05 × 0.16 × 0.48	0.20 × 0.24 × 0.26	0.32 × 0.16 × 0.04
data range (2θ, deg)	5–50	5–50	5–50
no. of data	3427	3527	3840
no. obsd. data ($F \geq 0.6\sigma(F)$)	2860	2569	2764
R_1	0.0422	0.0630	0.0680
R_2	0.0568	0.0586	0.0579
res density (e$^-$/Å^3)	+0.39/−0.30	+0.61/−0.42	+0.04/−0.33

Table II. Comparison of Important Bond Lengths and Angles (Å) for **1**, **3**, and **35**

VO-(SALIMH)-(Ca$^+$)	VO-(SHEDH)-(cat)[a,1]	VO-(SHEDH)-(HSHI)[a]	VO(SAL-IMH)-(ACAC)[a]	VO-(SHEDH)-(ACAC)[a,b]
V–O1, 1.59	V–O1, 1.60	V–O1, 1.61	V–O1, 1.64	V–O1, 1.60
V–O2, 1.91	V–O2, 1.90	V–O2, 1.90	V–O2, 1.98	V–O2, 1.97
V–O3, 1.91	V–O3, 1.88	V–O3, 1.85	V–O3, 1.97	V–O3, 1.99
V–O4, 2.20	V–O4, 2.15	V–O4, 2.12	V–O4, 2.20	V–O4, 2.15
V–N1, 2.15	V–N1, 2.11	V–N1, 2.09	V–N1, 2.05	V–N1, 2.05
V–N2, 2.11	V–N2, 2.20	V–N2, 2.17	V–N2, 2.10	V–N2, 2.19

[a] Numbering changed to reflect that of VO(SALIMH)(CAT). [b] There is a hydrogen bond between O5 (uncoordinated hydroxyl oxygen) and O3.

(12) Rehder, D.; Weidemann, C.; Duch, A.; Priebsch, W. *Inorg. Chem.* **1988**, *27*, 584.
(13) For review, see: (a) Mason, J. In *Multinuclear NMR*; Mason, J., Ed., Plenum Press: New York, 1987; Chapter 3. (b) Juranic, N. *Coord. Chem. Rev.* **1989**, *96*, 253. (c) Dechter, J. J. *Prog. Inorg. Chem.* **1985**, *33*, 393.
(14) (a) Ramsey, N. F. *Phys. Rev.* **1950**, *78*, 699. (b) Ramsey, N. F. *Phys. Rev.* **1952**, *86*, 243.
(15) (a) Mondal, J. A.; Schultz, F. A.; Brennan, T. D.; Scheidt, W. R. *Inorg. Chem.* **1988**, *27*, 3950. (b) Gheller, S. F.; Newton, W. E.; de Majid, L. P.; Bradbury, J. R.; Schultz, F. A. *Inorg. Chem.* **1988**, *27*, 359.

Experimental Section

Catechol, 3,5-di(*tert*-butyl)catechol, tetrachlorocatechol, 4-nitrocatechol, pyrogallol, salicylhydroxamic acid, acetohydroxamic acid, histamine dihydrochloride, *N*-(2-hydroxyethyl)ethylenediamine, 1,2-diaminopropane, and salicylaldehyde were purchased from Aldrich Chemical Co. and used as received unless otherwise noted. Both 3,5-dichlorosalicylaldehyde [3,5-Cl_2-SAL] and 5-bromosalicylaldehyde [5-Br-SAL] were obtained from Pfaltz and Bauer or Aldrich. The compounds VO_2(ENSAL),[17a] $[VO_2(HSHED)]_2$,[17b] and $V^{IV}O$(SALIMH)-ACAC[17c] were prepared as previously described. Abbreviations are given as ref 16, and the numbering scheme is provided in Table III.

Preparation of Complexes. Two general procedures were employed to prepare and isolate the VOLL′ complexes described in this study. The first was direct displacement of a terminal oxo ligand from a VO_2L complex by addition of a bidentate ligand such as catechol. The second was through addition of a bidentate ligand (e.g., catechol) to a vanadium(IV) precursor such as $V^{IV}O$(SALIMH)ACAC followed by air oxidation to the V(V) oxidation level.

Reaction of H_2L' with VO_2L. These reactions involved adding a stoichiometric amount of ligand H_2L' to the vanadium(V) starting material.

VO(ENSAL)CAT, 5. Catechol (recrystallized from benzene, 0.121 g, 1.10 mmol) and solid VO_2(ENSAL)[17a] (0.246 g, 1.0 mmol) were weighed into a 250-mL Erlenmeyer flask. Absolute ethanol was then added to bring the solution volume to 50 mL. The conversion of the yellow VO_2(ENSAL) to the purple/blue VO(ENSAL)(CAT), **5**, was rapid. The mixture was allowed to stir covered for 2 days after which time the purple reaction mixture was filtered, leaving a blue black solid on the filter. The solid was washed twice with cold (0 °C) absolute ethanol and then air-dried. A second crop of material was obtained when the filtrate was evaporated to dryness, washed with cold ethanol and air dried. This reaction is also successful using methanol or methylene chloride as the solvent. The total yield of **5** was 278 g (0.82 mmol, 82%): FAB(+) 339 $[M + 1]^+$, 338 $[M]^+$. Anal. Calcd for $C_{15}H_{15}O_4N_2V$: C, 53.27; H, 4.47; N, 8.28; V, 15.06. Found: C, 53.05; H, 4.48; N, 8.39; V, 14.5.

[VO(HSHED)(CAT)], 1. Catechol (0.11 g, 1.0 mmol) was added to a slurry of $[VO_2(HSHED)]_2$ (0.29 g, 1.0 mmol) and stirred in 100 mL of acetone. A deep purple solution resulted after 3 h. The volume was reduced to 50 mL by evaporation at reduced pressure. After filtering, 100 mL of hexane was added, and the solution was allowed to stand overnight at −20 °C. The dark microcrystalline precipitate was filtered, washed with hexane, and air-dried. X-ray quality crystals were obtained by slow evaporation of a methanol solution: yield 0.17 g (40%). Anal. Calcd for ($VC_{17}H_{19}N_2O_5$): C, 53.41; H, 5.01; N, 7.33. Found: C, 53.14; H, 4.99; N, 7.29.

[VO(HSHED)SHI], 35. Salicylhydroxamic acid (0.15 g, 1.0 mmol) was added to a slurry of $[VO_2(HSHED)]_2$ (0.28 g, 1.0 mmol) and stirred in 100 mL of acetone. A deep blue solution resulted after approximately 3 h. The volume was reduced to 50 mL by evaporation at reduced pressure. After filtering, 100 mL of hexane was added, and the solution was allowed to sit overnight at −20 °C. The dark microcrystalline precipitate was filtered, washed with hexane, and air-dried. X-ray quality crystals were obtained by slow evaporation of a methanol solution: yield 0.18 g (42%). Anal. Calcd for ($VC_{18}H_{20}N_3O_6$): C, 50.82; H, 4.74; N, 9.88. Found: C, 50.83; H, 4.64; N, 9.97.

Other complexes that were prepared and isolated as pure solids following these procedures include the following: **6**, **9**, **13**, **32**, **37**, and **39**.

Reaction of H_2L' with VOLL″. These reactions involved adding a stoichiometric amount of ligand H_2L' to the vanadium(IV) starting material ($V^{IV}O$(SALIMH)ACAC in most cases) with atmospheric oxygen serving as oxidant. Most complexes could be prepared in methanol, acetonitrile, or methylene chloride. Powders could be obtained either by slow evaporation of the reaction mixture by addition of a nonpolar cosolvent, usually ether or hexane. Hydroxamic acid complexes were prepared in a similar manner.

VO(SALIMH)(CAT), 3. In a typical preparation, $V^{IV}O$(SALIMH)ACAC·MeOH (0.51 g, 1.2 mmol) was dissolved in acetonitrile (50–100 mL). Catechol (0.15 g, 1.4 mmol) was added as a solid, and the solution was stirred overnight. Slow evaporation of the reaction mixture provided a purple powder (0.19 g, 31%). Average yield for several reactions: 62%. The X-ray quality crystals were obtained by slow evaporation of an acetonitrile/diethyl ether solution of the reaction mixture. FAB(+) 390 $[M + 1]^+$, 281 $[VO(SALIMH)]^+$; FAB(−) 389 $[M]^-$. Anal. Calcd for $C_{18}H_{16}N_3O_4V$: C, 55.54; H, 4.14; N, 10.79; V, 13.09. Found: C, 55.76; H, 4.32; N, 10.20; V, 13.3 ± 2.6.

VO(SALIMH)AHI, 40. $V^{IV}O$(SALIMH)ACAC (0.89 g, 2.2 mmol) was dissolved in 200 mL of methanol. Acetohydroxamic acid (0.16 g, 2.6 mmol) was added as a solid, and the solution was stirred overnight.

Table III. Chemical Shifts and Visible (λ_{E1}) and NIR (λ_{E2}) Transition Wavelengths for **1–41**

compound	chemical shift (ppm)	λ_{E1} (nm)	λ_{E2} (nm)
	CAT		
1 VO(HSHED)	221	530	870
2 VO(Br-HSHED)	283	532	867
3 VO(SALIMH)	480	540	920
4 VO(Br-SALIMH)	513	537	922
5 VO(ENSAL)	191	523	854
6 VO(Br-ENSAL)	256	526	860
7 VO(Cl_2-ENSAL)	324	531	869
8 VO(OMe-ENSAL)	168	517	849
	DBC		
9 VO(HSHED)	382	550	860
10 VO(Br-HSHED)	426	551	859
11 VO(SALIMH)	600	550	906
12 VO(Br-SALIMH)	604	547	906
13 VO(ENSAL)	345	545	853
14 VO(Br-ENSAL)	397	547	857
15 VO(Cl_2-ENSAL)	447	552	869
	TBC		
16 VO(HSHED)	−145	534	822
17 VO(Br-HSHED)	−97	533	846
18 VO(SALIMH)	−23	544	925
19 VO(Br-SALIMH)	25	551	940
	4-NC		
20 VO(HSHED)	−194		779
21 VO(Br-HSHED)	−159		795
22 VO(SALIMH)	−113		852
23 VO(Br-SALIMH)	−63		867
24 VO(ENSAL)	−232		766
	PYR		
25 VO(HSHED)	285	566	847
26 VO(Br-HSHED)	338	564	845
27 VO(SALIMH)	500	569	889
	TCC		
28 VO(HSHED)	−140	511	815
29 VO(Br-HSHED)	−90	528	850
30 VO(SALIMH)	0	531	931
31 VO(Br-SALIMH)	74	546	965
32 VO(ENSAL)	−213	508	819
33 VO(Br-ENSAL)	−129	546	811
34 VO(Cl_2-ENSAL)	0227	534	810
	SHI		
35 VO(HSHED)	−132		592
36 VO(SALIMH)	−73		630
37 VO(ENSAL)	−161		585
38 VO(Br-ENSAL)	−108		595
	AHI		
39 VO(HSHED)	−43		573
40 VO(SALIMH)	45		605
41 VO(ENSAL)	−66		565

(16) Abbreviations used and compound numbering scheme: HSALIMH = [4-(2-salicylideneaminato)ethyl]imidazole; Br-SALIMH = 4-[2-(5-bromosalicylideneaminato)ethyl]imidazole; H_2SHED = *N*-(salicylideneaminato)-*N*′-(2-hydroxyethyl)ethylenediamine; Br-H_2SHED = *N*-(5-bromosalicylideneaminato)-*N*′-(2-hydroxyethyl)ethylenediamine; HENSAL = *N*-(salicylideneaminato)ethylenediamine; HenSALBr = *N*-(5-bromosalicylideneaminato)ethylenediamine; Cl_2-HENSAL = *N*-(3,5-dichlorosalicylideneaminato)ethylenediamine; OMe-HENSAL = *N*-(4-methoxysalicylideneaminato)ethylenediamine; HACAC = 2,4-pentanedione; TBA = tetra-*n*-butylammonium cation; H_2CAT = catechol; H_2DBC = 3,5-di(*tert*-butyl)catechol, H_2TCC = tetrachlorocatechol, $H_2$4-NC = 4-nitrocatechol, H_2PYR = pyrogallol, H_3SHI = salicylhydroxamic acid, H_2AHI = acetohydroxamic acid.

(17) (a) Root, C. A.; Hoeschele, J. D.; Cornman, C. R.; Kampf, J.; Pecoraro, V. L. Submitted to *Inorg. Chem.* (b) Li, X.; Lah, M. S.; Pecoraro, V. L. *Inorg. Chem.* **1988**, *27*, 4657. (c) Cornman, C. R.; Kampf, J.; Lah, M. S.; Pecoraro, V. L. *Inorg. Chem.* **1992**, *31*, 2035.

The microcrystalline product was collected on a glass frit and dried under N_2 (0.64 g, 83%). FAB(+) 355 $[M + 1]^+$, 281 $[V^VO(SALIMH)]^+$; FAB(−) 354 $[M]^-$. Anal. Calcd for $C_{14}H_{15}N_4O_4V$: C, 47.47; H, 4.27; N, 15.82; V, 14.38. Found: C, 47.12; H, 4.42; N, 15.82; V, 15.0 ± 2.3.

The balance of the vanadium(V) complexes were prepared in situ and not isolated. In the in situ preparations, equal volumes of 5 mM solutions of $V^{IV}O$(SALIMH)ACAC, VO_2(ENSAL), VO_2(HSHED), and the appropriate salicylidenamine ring-substituted derivatives were reacted with the desired ligand L′, and the solutions were stirred for approximately 3 h before collecting the UV–vis–NIR and ^{51}V NMR spectra. Spectroscopic results for the fully characterized complexes were identical to those obtained for the same complexes prepared by the in situ method.

Collection and Reduction of X-ray Data. Suitable crystals of **1**, **3**, and **35** were obtained as described above. These crystals were mounted in glass capillaries. Intensity data were obtained at room temperature on a Siemans R3 diffractometer using Mo K_α radiation (0.7107 Å). Three standard reflections were measured every 97 reflections. Modified crystal and data parameters are given in Table I. Intensity data were collected using $\theta/2\theta$ scans. The data were reduced, the structures solved, and the model refined using the Siemans SHELEX PLUS program package.[18] Computations were carried out on a VAX Station 3500. In the subsequent refinement, the function $\sum w(|F_o| - |F_c|)^2$ was minimized where F_o and F_c are the observed and calculated structure factor amplitudes. The agreement indices $R_1 = \sum(|F_o - F_c|)/(\sum|F_o|)$ and $R_2 = [\sum(w|F_o - F_c|)^2/\sum w(F_o)^2]^{1/2}$ were used to evaluate the results. Atomic scattering factors are from *The International Tables for X-ray Crystallography*.[19] All hydrogen atoms, except the hydrogen attached to O6 of complex **35**, were located on a difference Fourier map and allowed to refine isotropically. The hydrogen on O6 was placed in a calculated position with d_{O-H} = 0.85 Å and $U(H) \approx 1.2U(eq)$ for O6. Unique data and final R indices are reported in Table I. Fractional atomic coordinates for **1**, **3**, and **35** are given in supplementary Tables S5, S11, and S17, respectively. Selected bond distances and angles for these compounds are provided in Table II.

Spectroscopic and Magnetic Measurements. Infrared spectra were obtained on a Nicolet 60-SX FT-IR as KBr pellets. Electronic spectra were recorded on a Perkin-Elmer Lambda 9 UV–vis–NIR spectrophotometer equipped with a Perkin-Elmer 3600 data station.

Fast atom bombardment (FAB) mass spectra were recorded on a VG 70-250-S mass spectrometer (VG Instruments, Manchester, UK). It was equipped with the standard VG FAB ion source and an Ion Tech Saddle-field atom gun. Xenon was used for the bombarding atom beam, with the atom gun controller set to 1 ma and 8 kV. 3-Nitrobenzyl alcohol was used as the FAB matrix.

The ^{51}V NMR spectra were collected using a Bruker AM200 instrument operating at 52.62 MHz and utilizing 8k or 16k data points over a 125 000 Hz spectral window. The data were collected on acetonitrile solutions (≥10 mM). Chemical shifts are reported in ppm versus $V^V(O)Cl_3$ (0 ppm) as an external standard and the error on the chemical shift is estimated to be ±1 ppm for resonances with a line width ≤1000 and ±3 ppm for resonances with line widths >1000 Hz. Typically, 1000 to 10 000 transients were acquired using a 90° pulse (14 μs) and no prepulse delay. The signal-to-noise ratio was improved via exponential multiplication of the FID which induced 10–100 Hz of line broadening.

Results and Discussion

Description of Structures. Other than simple VO^{3+} halides and esters (e.g., $VOCl_3$ or $VO(OCH_3)_3$), monooxovanadium(V) complexes are rare and few have been structurally characterized.[20] In particular, other than $V^{IV}O$(SALEN) and $V^VO(SALEN)^+$, there are no examples of VO^{2+} and VO^{3+} complexes with complete ligand sets common to both oxidation states. We were particularly interested in comparing the changes in the vanadium coordination sphere upon oxidation of the vanadium(IV) compounds containing imidazole since this represents a direct analogy to structural changes that may occur upon reduction of the active V(V) enzyme to the inactive V(IV) protein in vanadium bromoperoxidase. We have previously reported the molecular structures of $V^{IV}O$(SALIMH)L, where L = ACAC, salicylaldehyde anion, or SALIMH, and also the secondary amine containing $V^{IV}O$(HSHED)ACAC.[17b] In this contribution we can compare these vanadium(IV) materials with V^VO(HSHED)(CAT), **1**, V^VO(SALIMH)(CAT), **3**, and V^VO(HSHED)(HSHI), **35**. Important bond lengths for **1**, **3**, **35**, $V^{IV}O$(HSHED)ACAC, and $V^{IV}O$(SALIMH)ACAC are reported in Table II. ORTEP diagrams of compounds **1**, **3**, and **35** are presented as Figures 2 and 3, respectively.

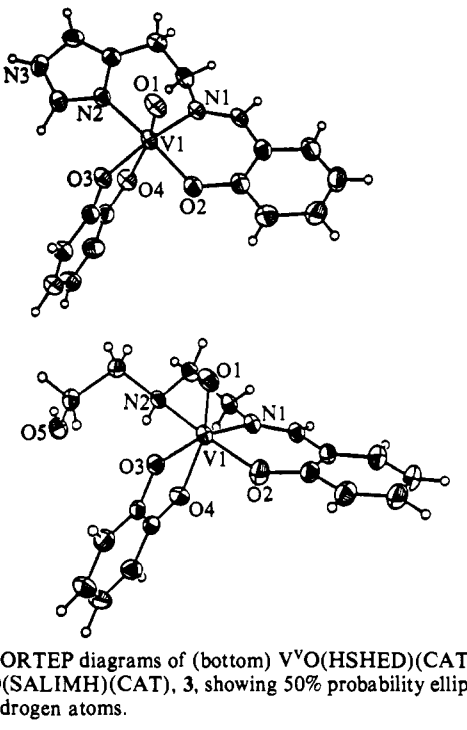

Figure 2. ORTEP diagrams of (bottom) V^VO(HSHED)(CAT), **1**, and (top) V^VO(SALIMH)(CAT), **3**, showing 50% probability ellipsoids for all non-hydrogen atoms.

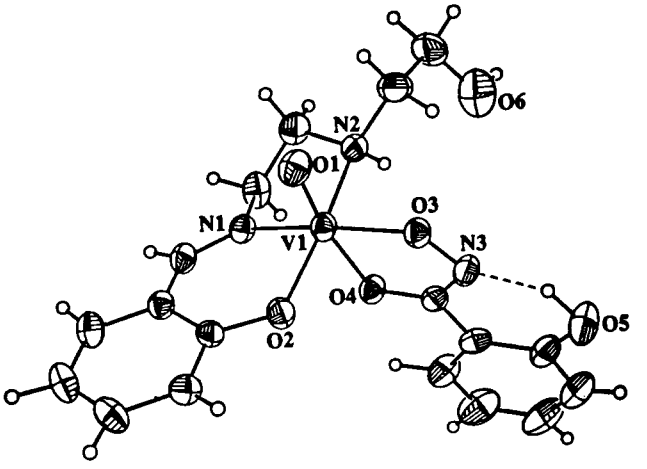

Figure 3. ORTEP diagram of V^VO(HSHED)(SHI), **35** showing 50% probability ellipsoids for all atoms.

There is surprisingly little variability in the vanadium-to-heteroatom distances across the five compounds. The terminal oxo-to-vanadium distance range is 1.59–1.64 Å; however, there is no significant oxidation state dependence. The only obvious trend is that the phenolate oxygen atoms (O2) and the in-plane oxygen atom (O3) of the bidentate ligand are significantly shorter in the vanadium(V) compounds. The latter effect may be due to the fact that the catecholate and hydroxamate ligands carry an extra negative charge. The vanadium–imine nitrogen atom (N1) distances are slightly *longer* in the vanadium(V) complexes reflecting the preference of the more highly oxidized centers for oxygen rather than nitrogen ligation. Most interestingly, there is essentially no difference in the vanadium–imidazole nitrogen (N2) bond distance between $V^{IV}O$(SALIMH)ACAC and V^VO(SALIMH)(CAT). The vanadium–imidazole N(2) distance in both the vanadium(IV) and vanadium(V) complexes is 2.1 Å

(18) SHELXTL PLUS; Copyright 1988, Siemens Analytical Instruments, Inc. Madison, WI.

(19) *International Tables for X-ray Crystallography*; Ibers, J., Hamilton, W., Eds.; Kynoch; Birmingham, England, 1974; Vol. IV, Tables 2.2 and 2.3.1.

(20) (a) Fisher, D. C.; Barclay-Peet, S. J.; Balfe, C. A.; Raymond, K. N. *Inorg. Chem.* **1989**, *28*, 4399. (b) Scheidt, R. W. *Inorg. Chem.* **1973**, *12*, 1758. (c) Knopp, P.; Weighardt, K.; Nuber, B.; Weiss, J.; Sheldrick, W. S. *Inorg. Chem.* **1990**, *29*, 363.

which is equivalent to the V–N distance (EXAFS data) reported for the native (vanadium(V)) and reduced (vanadium(IV)) forms of vanadium bromoperoxidase. Although the vanadium-to-imidazole distance is essentially invariant on oxidation-state change, there is a marked elongation in V–N2 when a secondary amine replaces the imidazole. In both the V(IV) and V(V) oxidation levels, the V–N(imidazole) distance is 0.06–0.09 Å shorter than that of the corresponding V–N(secondary amine). Thus, it would appear that imidazole is a better ligand to V(IV) and V(V) than secondary amines.

As with other metal complexes of catechol type ligands which have readily accessible semiquinone and quinone oxidation states, it is important to assign the relative oxidation states of the metal and ligand. Several vanadium complexes of catechols and semiquinones are reported in the literature. The important distances to be considered in these complexes are the vanadium–oxygen distance and the carbon–oxygen and carbon–carbon distances of the ligand. The vanadium–oxygen distance is indicative of the metal oxidation state (vide supra) and the carbon–oxygen and carbon–carbon distances are indicative of ligand oxidation levels. To the best of our knowledge, **1** and **3** represent the only structurally characterized examples of monooxovanadium(V) complexes of catechol. Therefore, comparisons to the "bare" vanadium(V) complexes of catechol in the literature should not be overinterpreted. However, if one considers the equatorial $V–O_{CAT}$ distance of 1.91 and 1.88 Å in **1** and **3**, respectively, it is found that these compare favorably with the average $V–O_{CAT}$ distances in the "bare" vanadium(V) complexes of Woolins and co-workers (1.91 and 1.93 Å)[21] and Peirpont and co-workers (1.91 Å).[22] The 1.90 Å average distance for **1** and **3** can be contrasted to the corresponding monooxovanadium(IV)–O_{CAT} distance of 1.96 Å for $K_2[VO(CAT)_2]$ reported by Cooper, Koh, and Raymond.[23] The range of C–O distances reported for vanadium–catechol complexes is 1.32–1.35 Å. The average C–O distances in **1** and **3** are 1.31 and 1.33 Å, respectively. The average C–C distances for the catechol rings in **1** and **3** are 1.39 Å which is consistent with an aromatic ring. Crystallographically characterized vanadium–semiquinone complexes have not been reported. Except for the relatively short C–O distance in **1**, all the structural information suggests that **1** and **3** are best formulated as vanadium(V)–catecholate complexes in the solid state. The short C–O distance in **1** may indicate a slight contribution of a semiquinone resonance form in this species. The discussion of catecholate versus semiquinone structural contributions will be continued below with respect to the NMR spectroscopy of these complexes.

One final structural comment is warranted on the $V^{V}O$(HSHED)(SHI). We have previously shown that the trianion of the salicylhydroxamic acid molecule can form ring structures called metallacrowns when SHI acts as a dinucleating unit with metals bound both to the hydroximate and iminophenolate functionalities.[24] In **35**, the ligand is a dianion and only the hydroximate group is bound. There is a strong internal hydrogen bond between the oxygen atom of the pendant phenol and the hydroximate nitrogen. An alternative and essentially indistinguishable formulation is to localize the proton on the hydroximate to form a hydroxamate and refer to the pendant group as a phenolate moiety. Based on the strength of the interaction of SHI with vanadium we prefer the first description; however, a combination of both models must be occurring. Raymond and coworkers have prepared and structurally characterized two vanadium complexes of alkyl hydroxamates in which the ligand is a monoanion.[20a] It should be noted that in these complexes, the second acidic proton has been replaced by the alkyl group. These structures contain two hydroxamate ligands, one of which is coordinated via the hydroxyl amine (η^1-bonding mode) to an equatorial site and by the carbonyl to the trans–axial coordination site in an analogous manner to **35**. The $vanadium–oxygen_{equatorial}$ bond distance is very comparable across the series of three compounds (1.85–1.88 Å). In contrast, the $vanadium–oxygen_{trans-axial}$ distance is 2.12 Å in **35** and 2.19 Å in the two Raymond complexes. This probably is a result of the change in charge between the hydroximate and hydroxamate ligands and indicates that the enol form of the hydroximate ligand has a stronger interaction with the monooxovanadium(V) center.

Scheme I

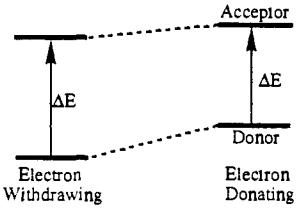

Electronic Spectroscopy of the Complexes. Dioxovanadium(V) complexes [e.g., VO_2(HSHED)] have strong UV transitions that lead to pale yellow solutions, while the vanadium(IV) complexes of the type $V^{IV}OLL'$ (e.g., $V^{IV}O$(SALIMH)ACAC) are pale red with weak d–d transitions in the visible spectrum. In contrast, all of the VO^{3+} complexes reported herein exhibit strong absorption bands, designated herein as E1, in the visible spectral region. As shown in Figure 4, the complexes containing catechol (or derivatives) show an additional band, designated as E2, in the near IR. Spectral parameters for these complexes are provided in Table III. Based on the intensity of the absorption, we assign these strong transitions as ligand-to-metal charge-transfer (LMCT) excitations.

Without the aid of resonance Raman spectroscopy, it is difficult to establish definitively whether the LMCT bands are phenolate-to-metal or catecholate-to-metal in origin in molecules such as VO(SALIMH)(CAT). Ideally, substitutions of either electron donating or withdrawing substituents on the catecholate or phenolate would produce corresponding changes (increasing or decreasing, respectively) in the charge-transfer energy of each band, E1 and E2, such that a definitive assignment can be made. If this were the case, one would assume that the donor was based on the substituted ligand. Unfortunately, the trends in energy upon substitution of these compounds are not this simple. In lieu of a definitive description of the orbitals involved in the charge-transfer transitions, the general trends observed for each substitution will be outlined below.

The visible band for the SHI complexes is always lower in energy than the corresponding transition for the AHI complexes. For the catechol complexes the LMCT donor set is predominantly localized on the catechol, while the acceptor orbitals are metal centered (d_{xz}, d_{xy}, or d_{yz}). This assignment is supported by the energy trends of the LMCT upon catechol substitution: For the E1 band the energy trend is PYR < DBC < CAT ≈ TBC ≈ TCC (<4-NC assuming this complex has a higher energy LMCT transition in the UV region). For the E2 band, the energy trend is dominated by the presence of the SALIMH ligand, as discussed below. Excluding the VO(SALIMH)L′ data, the energy trend for E2 is CAT < DBC < PYR ≈ TBC < TCC < 4-NC. That the transition energies for the catechols with electron donating substituents are, in general, lower than the transition energies for the catechols with electron withdrawing substituents is consistent with the bidentate ligand having a significant influence on the donor orbital as shown in Scheme I. Electron withdrawing phenolate substituents tend to *decrease* the LMCT energy, E1, while no general trend is observed for the effect of phenolate substitution on E2 (again, excluding the SALIMH data). This result indicates that the phenolate substitution must have a dominant effect on the metal localized acceptor orbital and a much smaller influence on the donor orbital since one would expect E1 to increase if electron withdrawing substituents are important to the donor orbital.

(21) (a) Kabanos, T. A.; White, A. J. P.; Williams, D. J.; Woollins, J. D. *J. Chem. Soc., Chem. Commun.* **1992**, 17. (b) Kabanos, T. A.; Slawin, A. M. Z.; Williams, D. J.; Woollins, J. D. *J. Chem. Soc., Chem. Commun.* **1990**, 193.

(22) Cass, M. E.; Gordon, N. R.; Pierpont, C. G. *Inorg. Chem.* **1986**, *25*, 3962.

(23) Cooper, S. R.; Koh, Y. G.; Raymond, K. N. *J. Am. Chem. Soc.* **1982**, *104*, 5092.

(24) Lah, M. S.; Pecoraro, V. L. *Comments Inorg. Chem.* **1990**, *11*, 59.

In the course of these studies, we observed an interesting trend related to imidazole ligation. The energy of the near IR band, E2, is dominated by the presence of the SALIMH ligand such that the nine lowest energy transitions correspond to VO(SALIMH) and VO(BrSALIMH) complexes with an energy order: TCC < TBC < CAT < DBC < PYR. The reasons for this order, which is opposite of that predicted from Scheme I, are complex and unclear at this time; however, the observations are consistent with a model in which the acceptor orbital (influenced by the coordinated imidazole and catechol substitution) is lowered in energy to a greater extent than the corresponding donor orbital (influenced predominantly by catechol ring substitution).

In summary, the donor orbitals for the LMCT bands have dominant contributions from the bidentate ligand as is observed for many transition-metal–catechol complexes. These conclusions are consistent with findings for the homoleptic complexes $[V^V(CAT)_3]^-$ and $[V^V(DBC)_3]^-$ in which both a low- and high-energy LMCT band are reported.[23] The vanadium(V) phenolate complexes reported to date which do not contain coordinated noninnocent ligands have electronic transitions at energies higher than the E2 bands reported for these catecholate complexes.[25]

Vanadium-51 NMR Spectroscopy. Vanadium-51 NMR has been increasingly utilized to probe the electronic environment of biologically relevant V(V) compounds. The majority of compounds with exclusively oxygen and nitrogen ligation fall far upfield of the standard $VOCl_3$ in the general region of −400 to −700 ppm. Exceptions include bare V(V) compounds such as $V^V(N_2S_3)$(DBC)(phenanthroline) at +780 ppm.[21b] The remaining complexes with downfield chemical shifts are halide or sulfur containing species.[12] Rehder has presented a referencing scale based on a correlation of ^{51}V NMR shifts with $\sum\chi$, the sum of the coordinated heteroatom electronegativities (using the Zhang formalism[26]), for a wide variety of V(V) complexes with coordination numbers 4–6.[12] A carboxylate rich, six- or seven-coordinate structure for the active site of vanadium bromoperoxidase has been proposed based on this correlation in which the carboxylate ligands are probably bound in an η^2 manner.

While this correlation effectively predicts the chemical shift range for most complexes of VO_2^+ and VO^{3+}, it is less effective in describing materials that have coordinated noninnocent ligands. Based on the heteroatom electronegativities tabulated by Zhang, one would calculate a $\sum\chi = 20.69$ for **1** and **35** and $\sum\chi = 17.05$ for **43**. Applying these values to the Rehder referencing scale would predict δ values in the upfield region between −480 and −600 ppm. In contrast, the chemical shift range for the complexes of V^VOLL' (where L = SALIMH, HSHED, ENSAL, and their phenolate ring substituted derivatives and L′ = catecholate and derivatives, salicylhydroxamic and acetohydroxamic acids or a terminal oxo moiety) extend over a remarkable 1130 ppm including downfield shifts to +604 ppm. Apparently a new correlation is required to describe chemical shifts of complexes with noninnocent type ligands. It will be shown below that these marked deviations from the predictions based on electronegativity values are a direct consequence of the coordination of noninnocent ligands to the VO^{3+} unit and that the magnitude of the downfield shift correlates with the LMCT energies in complexes with electronically similar noninnocent ligands. Chemical shifts for complexes **1**–**41** are provided in Table III.

The progressive downfield shift of the ^{51}V NMR resonances is illustrated by the spectra of VO_2(ENSAL), **44** VO(ENSAL)(TCC), **32**, VO(ENSAL)(CAT), **5**, and VO(ENSAL)(DBC), **13**, which are presented in Figure 5 from top to bottom, respectively. The VO_2^+ complex, **44**, has a single resonance at −555 ppm. This shift is typical for dioxovanadium(V) complexes of oxygen/nitrogen ligands (e.g., VO_2(HSHED) −529 ppm; VO_2(HSALIM) −542 ppm) and conforms well with the previously described electronegativity correlation. However, increasingly

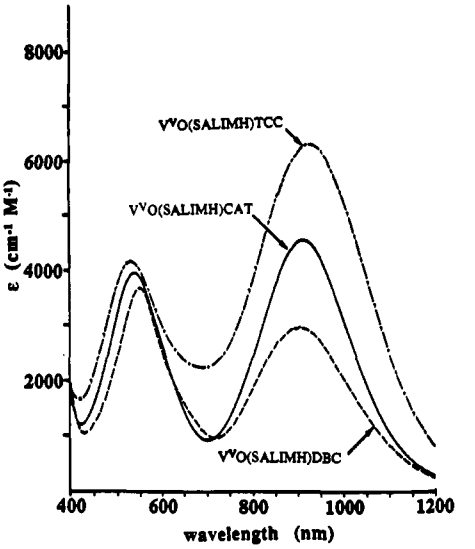

Figure 4. UV–vis near-IR spectra of VO(SALIMH)TCC, **30**, VO(SALIMH)CAT, **3**, and V^VO(SALIMH)DBC, **11**, in CH_3CN.

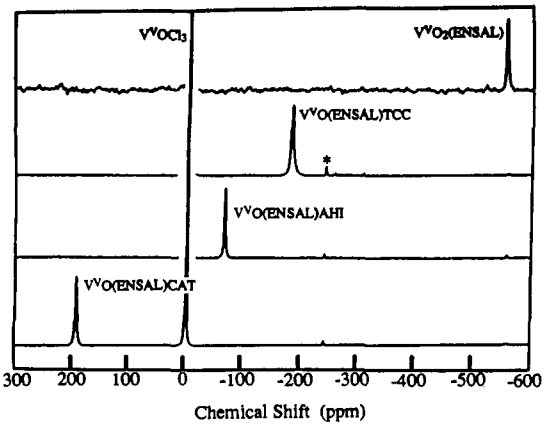

Figure 5. ^{51}V NMR spectra of acetonitrile solutions of (from top to bottom) VO_2(ENSAL), **44**, VO(ENSAL)TCC, **32**, VO(ENSAL)CAT, **5**, and VO(ENSAL)DBC, **13**. All spectra collected at 52.62 MHz and referenced to external $VOCl_3$. The asterisk denotes an impurity in the external standard.

downfield shifted resonances appear as more electron rich catechols are substituted for the terminal oxo moiety. Examination of Table III indicates that similar trends are observed for the HSHED and SALIMH complexes.

Analysis of the Chemical Shift Based on the Paramagnetic Shielding Factor. The chemical shift, δ, is related to the shielding constant, σ, through eq 2a where δ is the chemical shift of the nucleus of interest, σ_{ref} and σ are the shielding constants for a

$$\delta = (\sigma_{ref} - \sigma)/(1 - \sigma_{ref}) \quad (2a)$$

$$\delta \approx (\sigma_{ref} - \sigma) \quad (2b)$$

reference compound ($VOCl_3$ for vanadium) and the compound of interest, respectively. If one assumes $\sigma_{ref} \ll 1$, then the approximation in eq 2b is valid. The general theoretical description of the shielding constant, σ, as presented by Ramsey for nuclei without unpaired spin, indicates that σ equals the sum of a diamagnetic and paramagnetic term, σ^d and σ^p, as shown in eq 1 ($\sigma = \sigma^p + \sigma^d$).[14] In the presence of nuclei with unpaired spin, the equation for total shielding would require a third term to account for the local field at the observed nucleus which is induced by the unpaired spin.[27]

Since the primary contribution to σ^d is from core electrons of the nucleus being observed, and, to a much lesser extent, the

(25) (a) Bonadies, J. A.; Butler, W. M.; Pecoraro, V. L.; Carrano, C. J. *Inorg. Chem.* **1987**, *26*, 1218. (b) Dutton, J. C.; Murray, K. S.; Tiekink, E. R. T. *Inorg. Chim. Acta* **1989**, *166*, 5.

(26) Zhang, Y. *Inorg. Chem.* **1982**, *21*, 3886.

(27) *NMR of Paramagnetic Molecules*; LaMar, G. N., Horrocks, W. DeW., Holm, R. H., Eds. Academic Press: New York, 1973.

electrons of neighboring atoms, the diamagnetic component of the total shielding is essentially constant for any one nucleus, and for vanadium it is approximately equal to the free atom value of 1710 ppm.[28] The paramagnetic term describes the mixing of excited states, $|n\rangle$, into the ground state, $\langle 0|$, of the molecule in the presence of a magnetic field as shown in eq 3 where r_{kN} is the position vector for the kth electron with respect to the nucleus being observed, l_{kN} is the kth component of the angular momentum

$$\sigma^p = -(\mu_0/4\pi)(e^2/2m^2)[\sum_{n\neq 0}(E_n - E_0)^{-1}\{\langle 0|\sum_k r_{kN}^{-3} l_{k,N}|n\rangle \langle n|\sum_k l_k|0\rangle + \langle 0|\sum_k l_k|n\rangle\langle n|\sum_k r_{kN}^{-3} l_{k,N}|0\rangle\}] \quad (3)$$

operator with respect to the observed nucleus, l_k is the angular momentum operator with respect to the chosen origin, and the other terms have their usual meanings.[13a] It should be noted that this is a general equation that takes the sum over all molecular states which transform via the angular momentum operator. While eq 3 may be useful for small systems such as dihydrogen, the lack of accurate wave functions for larger molecules decreases the utility of this equation for calculating reasonable shielding factors.

Since the paramagnetic shielding is affected predominantly by the electronic structure of the nucleus being observed (r^{-3} dependence), Saika and Slichter have approximated the total shielding to be the sum of the local diamagnetic and paramagnetic contributions and a nonlocal term as shown in eq 4 where σ^d_{local}

$$\sigma_{local} = \sigma^d_{local} + \sigma^p_{local} + \sigma_{nonlocal} \quad (4)$$

represents the "diamagnetic correction *for the atom in question*", σ^p_{local} represents "the contribution from magnetic fields set up by the orbital motion of the valence orbitals" for the atom in question, and $\sigma_{non\text{-}local}$ represents the contribution from closed shell and valence orbitals of other atoms.[29] For most coordination complexes, $\sigma_{nonlocal}$ is relatively small and therefore need not be evaluated. Since the diamagnetic contribution is essentially constant, the major contributor to chemical shift is σ^p_{local}.

Griffith and Orgel have evaluated the local paramagnetic shielding for low-spin octahedral cobalt(III) complexes[30] in terms of crystal field theory in the strong field limit. The most recent revision of the crystal field treatment of σ^p has been presented by Bramley and co-workers for molecules of high symmetry (O_h, C_{4v}, D_{4d}) using an intermediate field approach and is shown in eq 5 where $^1A_{1g}$ and $^1T_{1g}$ are the ground and excited states mixed by the angular momentum operator L_z, $\langle r_{3d}^{-3}\rangle$ is the expectation

$$\sigma^p_{local} = -[(\mu_0 e^2/12\pi m_e)\langle r_{3d}^{-3}\rangle\beta^{-1}][\beta\sum_{k=x,y,z}|\langle {}^1A_{1g}|L_z|{}^1T_{1g}\rangle|^2/E({}^1T_{1g}(k))] \quad (5)$$

value for the inverse cube of the radius of a 3d orbital, E is the energy difference between the $^1A_{1g}$ and $^1T_{1g}$ electronic states, and β is the nephelauxetic ratio.[31] As shown by the determination of γ_0 for cobalt complexes, this approach is quantitatively valuable for low-spin d^6 systems of relatively high symmetry.

The complexes reported herein are high valent (d^0) and of low symmetry (pseudo C_s), and the electronic transitions are dominated by LMCT transitions. Since vanadium(V) has no valence electrons, the local contribution to the paramagnetic shielding, as defined by Saika and Slichter, is zero. Therefore, the large chemical shift range for these vanadium complexes of noninnocent ligands must be due to the nonlocal term of eq 4. In the general context of the Ramsey equation, this point is one of semantics

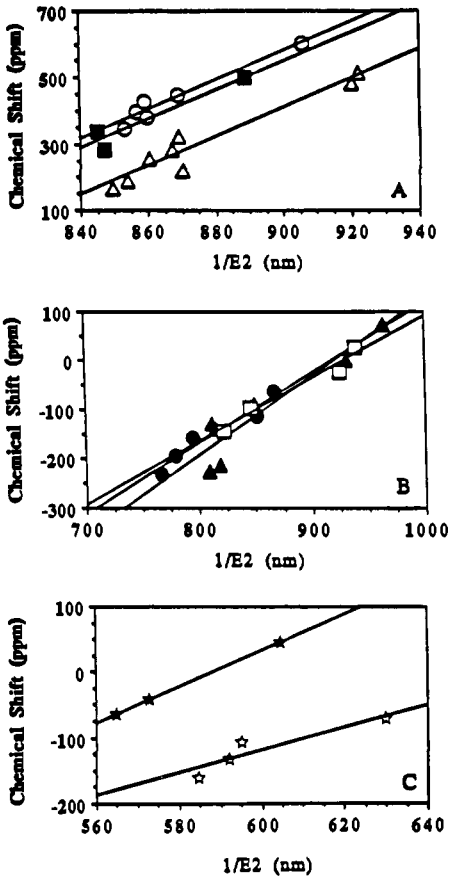

Figure 6. Correlation between ^{51}V NMR chemical shift and 1/E2 for VOLL′ complexes according to bidentate ligand, L′. Plots A, B, and C are for catechols with electron donating substituents and catechols with electron withdrawing substituents and hydroximates, respectively. Note that the axes are different for each plot. The symbols denote the following bidentate ligand series: CAT, DBC, PYR, TCC, 4-NC, TBC, SHI, AHI.

since all transitions are considered; however, the effect of LMCT transitions on the paramagnetic term of eq 1 are rarely considered explicitly since they are of high energy and thus would have a small effect relative to d–d transitions. Schultz and co-workers have described this relationship for ^{95}Mo chemical shifts and the energy of LMCT transitions in molybdenum–catechol complexes.[15]

We have evaluated the nonlocal term for the vanadium complexes by analogy to the treatment of Bramley for the local paramagnetic shielding as discussed above. Given the low symmetry of these complexes, all transitions will transform as the angular momentum operator, and therefore the LMCT transitions should produce a sizeable shielding of the vanadium-51 nucleus. For the discussion at hand, the relationship between the paramagnetic shielding and the energy of the LMCT transition is adequately described by eq 6, where B represents the matrix elements of eq 3 and ΔE represents the energy of the transition. Since the complexes to be analyzed are essentially isostructural, it is expected that B is nearly constant for any series of bidentate ligands.

$$\sigma^p = -B/\Delta E \quad (6)$$

Since σ^p is not an observable parameter, we have combined eqs 1, 2b and 6 to obtain the relationship between the chemical shift and the shielding factor as shown in eq 7. From eq 7 it follows that a plot of δ versus $1/\Delta E$ should yield a line with a positive slope of magnitude B and an intercept (at $1/\Delta E = 0$) which is the paramagnetic shielding of the reference. If σ^p_{ref} and δ are known, the total shielding for the vanadium nucleus can be calculated from eq 2b, and thus an absolute shielding scale may be formulated.

$$\delta = \sigma^p_{ref} + B/\Delta E \quad (7)$$

(28) We have chosen to use the value of σ^d = 1710 ppm for the free vanadium atom as calculated by Dickinson. This value is intermediate between those reported by Rehder and co-workers for complexes of vanadium-(1+) (1712 ppm) and Nakano for vanadate (1708 ppm). (a) Dickinson, W. C. *Phys. Rev.* **1950**, *80*, 563. (b) Schmidt, H.; Rehder, D. *Transition Met. Chem.* **1980**, *5*, 214. (c) Nakano, T. *Bull. Chem. Soc. Jpn.* **1977**, *50*, 661.

(29) Saika, A.; Slichter, C. P. *J. Chem. Phys.* **1954**, *22*, 26.

(30) (a) Griffith, J. S.; Orgel, L. E. *Trans. Faraday Soc.* **1957**, *53*, 601. (b) Griffith, J. S. *The Theory of Transition Metal Ions*; Cambridge University Press: Cambridge, 1961.

(31) Bramley, R.; Brorson, M.; Sargeson, A. M.; Schaffer, C. E. *J. Am. Chem. Soc.* **1985**, *107*, 2780.

Plotting δ versus $1/\Delta E$ for the monooxovanadium(V) complexes according to the derivatives of the tridentate ligands ENSAL, HSHED, and SALIMH yields three nonlinear groups of data which correspond to complexes of hydroximates, catechols with electron donating substituents, or catechols with electron withdrawing substituents. This result indicates that the assumptions of eq 6 are not valid when the complexes are grouped according to tridentate ligand type. However, replotting the data according to bidentate ligand type as suggested by the above analysis, one obtains the linear relationships shown in Figures 6A–C for complexes of electron donating catecholates, electron withdrawing catecholates, and hydroximates, respectively. While it is clear that the energy of the LMCT correlates with the downfield chemical shift,[32] the different slopes for the three families of lines indicate that the factor B of eq 6 also contributes to the shielding of the vanadium nucleus. The B dependence of the chemical shift is obvious when one compares the chemical shifts for the hydroximate complexes to the chemical shifts obtained for the complexes of electron withdrawing catecholates. As seen in Figure 6 (parts B and C), the chemical shift for these two series are quite similar even though the charge-transfer energy is very different. According to Ramsey theory, one would predict very different chemical shifts for these compounds if B were indeed comparable for the two series. As this is not the case, it is concluded that B for the hydroximate complexes is smaller than the B for the catecholate complexes with electron withdrawing substituents.

Absolute Shielding Scale. From eq 2b the total shielding of a nucleus can be obtained if one knows the chemical shift and the total shielding of the reference, σ_{ref}. The reference shielding term can be obtained from eq 1 ($\sigma_{ref} = \sigma^{d}_{ref} + \sigma^{p}_{ref}$) where σ^{p}_{ref} is extrapolated from plots of eq 6 and $\sigma^{d} \approx 1710$ ppm. Since σ^{p} is expected to be negative we can set an upper limit for σ^{p}_{ref} of $\sigma^{p}_{ref} \leq -1963$ ppm.[33] Figure 7 presents plots of δ vs $2/(E1 + E2)$. The average energy approximation has been used for these plots since all low-energy transitions involving metal orbitals should be utilized according to Ramsey theory in which the sum of all appropriate transitions is utilized. In this case, since values for B are not known, we have taken the average energy. Extrapolating the plots to $2/(E1 + E2) = 0$, it is apparent that the intercept is not constant, as predicted by eq 6. The intercepts for the complexes of CAT, DBC, and PYR are spread over ≈3000 ppm (−6000 to −9000 ppm). Other studies have been presented in which the extrapolated intercept is not constant. Verkade and Weiss have reported different lines (with disparate intercepts) for cobalt complexes with ligands from different rows of the periodic table.[34] Shultz and co-workers have made similar observations for molybdenum complexes of noninnocent ligands.[15] In the case of the cobalt(III) compounds this observation has been attributed to the "cloud expanding" ability of the third and fourth row donor atoms. The average intercept for the complexes of TCC and TBC is at $\sigma^{p}_{ref} = -2130$ ppm; a value which is consistent with the predicted upper limit for σ^{p}_{ref}.[38]

We see two possible explanations for the range of intercepts observed. First, the factor B may not be a constant for any series of complexes, i.e., B for $V^{V}O$(ENSAL)CAT may be different than B for $V^{V}O$(HSHED)CAT. If this is the case, then B would need to be evaluated for each complex and an independent line drawn in each case. This is conceptually analogous to applying a β factor as described by Bramley. Since only the tridentate ligand is varied for any series of complexes, it is unlikely that the variation in B is significant. Examination of the crystallographic data for several complexes of ENSAL, HSHED, and SALIMH indicate that the bond distances do not change substantially upon changing the tridentate ligand (see Table II). Second, some of these complexes, in particular the complexes of CAT, PYR, and DBC, may have a small but significant vanadium(IV)–semiquinone contribution to the ground state. If this is the case, the shielding may have a temperature dependent paramagnetic term, σ^{TDP}, which would need to be included in the total shielding. Therefore, the intercept for these compounds would equal $\sigma^{p}_{ref} + \sigma^{TDP}$, not just σ^{p}_{ref}. This explanation is qualitatively appealing since metal reduction is the extreme limit of ligand-to-metal charge transfer. The broad resonances observed for $V^{V}O$(SALIMH)CAT and $V^{V}O$(SALIMH)DBC (2000–4000 Hz) indicate that relaxation of the vanadium nuclear spin is more rapid in these complexes than observed in the complexes of hydroximates or electron withdrawing catecholates. This enhanced relaxation of the nuclear spin may be a result of interactions between the nuclear spin and the unpaired electron spin in the vanadium(IV)–semiquinone ground state.[36]

Based on $\sigma^{p}_{ref} = -2130$ ppm, we propose the shielding scale shown in Figure 8. Importantly, all reported chemical shifts for vanadium complexes are downfield (deshielded) relative to $\sigma^{d} = 1710$ ppm (the right hand border of the plot). Also, the calculated σ^{p} values for $V(CO)_6^-$ and $CpV(CO)_3THF$ are −165 and −2023 ppm, respectively, values which compare favorably with those reported by Jameson, Rehder, and Hoch (−500 and −2500 ppm) based on the relationship between the chemical shift, δ, and the

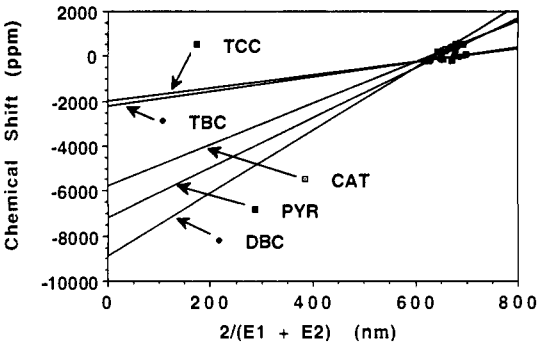

Figure 7. Correlation between ^{51}V NMR chemical shift and the inverse of the average energies of E1 and E2 for complexes which have both visible and near-IR transitions.

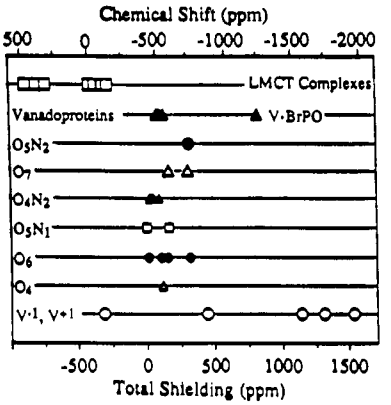

Figure 8. Absolute shielding scale for vanadium indicating the absolute shielding of the LMCT complexes reported in this paper as well as the absolute shielding for the vanadium substituted proteins RNase T1 (δ = −516 ppm),[38] phosphoglycerate mutase (δ = −560 ppm),[39] and transferrin ($\delta \approx -530$ ppm for both signals);[11] four-, six- and seven-coordinate complexes of O and N donors (as compiled by Rehder);[12] and low valent vanadium(1−) and vanadium(1+) complexes.[40]

(32) The R^2 values for the lines plotted in Figures 6A–C are SH1, 0.837; AH1, 1.000; CAT, 0.935; DBC, 0.969, PYR, 0.924; TCC, 0.879; 4-NC, 0.945; TBC, 0.966. The standard error for the intercept of the lines, as acquired from the program Cricketgraph, is ±200 ppm.

(33) From eq 2b ($\delta \cong \sigma^{p}_{ref} - \sigma^{p}$): If $\sigma^{p} \leq 0$, then $\sigma^{p}_{ref} \leq \delta$. The highest field chemical shift (i.e., smallest paramagnetic shielding) is reported as δ = −1963 ppm; therefore, $\sigma^{p}_{ref} \leq -1963$ ppm.

(34) Weiss, R.; Verkade, J. G. *Inorg. Chem.* **1979**, *18*, 529.

(35) We have also prepared the series $V^{V}O$(benzohydroxamate)X where X = F, Cl, Br. These complexes have charge-transfer transitions in the visible region of the spectrum and an intercept of ≈−2100 ppm.

(36) For the complexes **3** and **11** (and possibly others of the SALIMH series with electron donating substituents on the catechol) there is an observable EPR signal. We believe this is an impurity and not representative of the ground state (or excited state) of the molecule since variations in the concentration of the EPR active species do not significantly affect the chemical shift or line width.

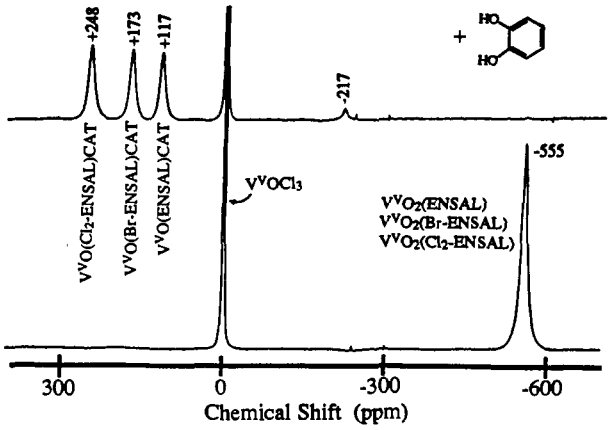

Figure 9. Chemical shift dispersion induced by coordination of catechol to VO_2L complexes: (bottom) ^{51}V NMR spectrum of an equimolar mixture of VO_2(ENSAL), VO_2(Br-ENSAL), and $VO_2(Cl_2$-ENSAL) and (top) ^{51}V NMR spectrum of the solution obtained after addition of H_2CAT to the solution responsible for the bottom trace. Spectra were recorded on DMSO-d_6 solutions. The −217 ppm resonance is tentatively assigned to $[V^VO(CAT)_2]^-$ which may form with the slight excess of catechol in solution.

temperature dependence of the chemical shielding, $d\sigma/dT$.[38] Nakano[28c] has calculated a paramagnetic shielding value of σ^P for $KV(CO)_6$ which is approximately an order of magnitude larger than that reported here and by Jameson et al.

Effect of Tridentate Ligand Substitution on Chemical Shift. It is interesting to note that for any series of bidentate ligands, the chemical shift for the complexes of SALIMH (imidazole ligation) are always downfield of the chemical shifts for complexes of both HSHED and ENSAL. This is consistent with a decrease in ΔE for the imidazole complexes relative to the amine complexes as discussed above.

The range of chemical shifts observed for any single noninnocent ligand complex is considerably greater than that for complexes of noninnocent ligands such as the V^VO_2(TRIDENTATE) series. An example of this difference is illustrated in Figure 9 in which trace A is for an equimolar mixture of V^VO_2(ENSAL), V^VO_2(BrENSAL), and $V^VO_2(Cl_2$ENSAL) in DMSO. The single resonance for this mixture indicates that σ^P is quite insensitive to substitutions on the equatorial phenolate ligand. Addition of approximately 1.2 equiv of catechol to the solution in trace A results in the formation of the corresponding catecholato complexes V^VO(ENSAL)CAT, V^VO(BrENSAL)CAT, and $V^VO(Cl_2$ENSAL)CAT which are responsible for trace B in Figure 9. The chemical shift range for these three complexes is 131 ppm showing that σ^P becomes very sensitive to equatorial phenolate substitution. Thus, catechol substitution provides a "spectroscopic magnifying glass" which enables one to resolve by ^{51}V NMR spectroscopy minor changes in the electronic structure of the vanadium center. In this regard, the addition of catechol is analogous to the use of paramagnetic shift reagents in ^1H and ^{13}C NMR, the latter being a temperature dependent paramagnetic shift reagent and the former being a temperature independent paramagnetic shift reagent (with possible TDP contributions).

The order of the chemical shifts for V^VO(ENSAL)CAT, V^VO(BrENSAL)CAT, and $V^VO(Cl_2$ENSAL)CAT in trace B of Figure 9 provides some insight into the bonding in these complexes. If the equatorial phenolate contributes to the energy of the donor orbital, then one would expect the dichloro substituted complex, $V^VO(Cl_2$ENSAL)CAT, to have the largest ΔE and the highest field (less positive chemical shift). In contrast, the unsubstituted complex, V^VO(ENSAL)CAT, should have the lowest field (most positive chemical shift) since ΔE should be smaller in the absence of electron withdrawing substituents. In fact, the opposite order is observed. This suggests that the phenolato ligand must contribute predominantly to the acceptor orbital, and the donor orbital must be predominantly of catecholate or hydroximate character. This is also consistent with the trends found upon catechol substitution.

Conclusion

In this paper we have shown that vanadium complexes of nitrogen and oxygen ligands can have ^{51}V NMR chemical shifts which are significantly downfield of the "normal" shift range for these compounds based on empirical relationships. The dominant factor in the deshielding of these compounds is the low-energy ligand-to-metal charge-transfer transitions which are directly associated with the presence of noninnocent ligands such as catecholate or hydroximate. The magnitude of the deshielding is inversely proportional to the energy of the LMCT. Anomalous intercepts for plots of δ versus $1/\Delta E$ for the complexes of ligands with high energy occupied molecular orbitals may indicate a temperature dependent contribution to the chemical shielding.

An absolute shielding scale which is consistent with all reported chemical shifts has been proposed. From this scale it is clear that the vanadium bromoperoxidases have a smaller temperature independent paramagnetic shielding ($\sigma^P \approx -1100$) than most complexes of vanadium(V) and that noninnocent ligands of the type examined here are almost certainly not involved in the metal coordination sphere in this enzyme. We have shown that imidazole ligation deshields the vanadium nucleus in vanadium complexes of catechols and hydroxamic acids. This may not be true for other ligand sets. The novel spectroscopy of these complexes may be relevant to the solution characterization of vanado-biomolecules such as complexes of ion sequestering agents based on hydroxylamines, catechols, or pyrogallol moieties.

Acknowledgment. The authors acknowledge the initial synthesis of VO_2(ENSAL) and many useful conversations on this topic with Prof. Charles Root. This work was supported by the NIH (Grant GM 42703 to V.L.P.) and an NIH Postdoctoral Fellowship to CRC (Grant GM14188).

Supplementary Material Available: Tables of fractional atomic coordinates, anisotropic thermal parameters of all non-hydrogen atoms, fractional atomic positions for hydrogen atoms, a complete set of bond distances, and a complete set of bond angles for **1**, **3**, and **35**, respectively, and Figures 10–12 of complete numbering schemes for all atoms in **1**, **3**, and **35** (18 pages); list of observed and calculated structure factors (34 pages). Ordering information is given on any current masthead page.

(37) Jameson, C. J.; Rehder, D.; Hoch, M. *J. Am. Chem. Soc.* **1987**, *109*, 2589.

(38) Rehder, D.; Holst, H.; Quaas, R.; Hinrichs, W.; Ulrich, H.; Saenger, W. *J. Inorg. Biochem.* **1989**, *37*, 141.

(39) Stankiewicz, P. J.; Gresser, M. J.; Tracey, A. S.; Hass, L. F. *Biochemistry* **1987**, *26*, 1264.

(40) Rehder, D. *Bull. Magn. Reson.* **1982**, *4*, 33.